AgriEngineering

Article

A DisDAQ-Based Mobile Sensor System for Multi-Level Spectral Monitoring of Vineyard Canopy

Leander B. Hörmann [1,*], Florian Hammer [1], Tamás Deák [2], Róbert Oláh [2], Diána Ágnes Nyitrainé Sárdy [2], Balázs Nagy [2], Richard Schmidt [1], Reinhard Ritter [1], Luca Masiero [3], Patrick Marcuzzo [3] and Péter Bodor-Pesti [2]

[1] Linz Center of Mechatronics GmbH, Altenberger Strasse 69, 4040 Linz, Austria; florian.hammer@lcm.at (F.H.); richard.schmidt@lcm.at (R.S.); reinhard.ritter@lcm.at (R.R.)
[2] Institute for Viticulture and Oenology, Hungarian University of Agriculture and Life Sciences, Villányi Street 29-43, H-1118 Budapest, Hungary; deak.tamas@uni-mate.hu (T.D.); olah.robert@uni-mate.hu (R.O.); nyitraine.sardy.diana.agnes@uni-mate.hu (D.Á.N.S.); nagy.balazs@uni-mate.hu (B.N.); bodor-pesti.peter@uni-mate.hu (P.B.-P.)
[3] Research Centre for Viticulture and Enology, CREA Council for Agricultural Research and Economics, via XXVIII aprile 26, 31015 Conegliano, Italy; luca.masiero@crea.gov.it (L.M.); patrick.marcuzzo@crea.gov.it (P.M.)
* Correspondence: leander.hoermann@lcm.at

Abstract

Remote and proximal sensing methods are widely applied in agriculture and viticulture to monitor plant health, water status, yield, and quality. In this study, we introduce a mobile sensor system comprising normalized difference vegetation index (NDVI) sensors, photochemical reflectance index (PRI) sensors, an RGB camera, and a GPS tracking module. Commercially available sensors were integrated into a dedicated DisDAQ data acquisition system to enable continuous, georeferenced measurements. NDVI and PRI sensors measured canopy reflectance at three levels: the top of the canopy (TC), upper canopy section (UCS), and lower canopy section (LCS), complemented by environmental reference sensors. Test runs were conducted in eight rows covering approximately 1.32 km in Hungary in June 2025. NDVI and PRI measurements were acquired alternately, with a minimum spatial sampling interval of approximately 0.57 m along the vineyard rows without any sensor data loss. Statistical evaluation assessed local and vertical variability using absolute differences between vegetation index measurements, Kruskal–Wallis tests with Bonferroni-corrected Dunn's post hoc comparisons, and Shannon entropy. Results showed significant differences in both NDVI and PRI values among canopy sections. Median NDVI values were 0.4329, 0.3221 and 0.6161, while median PRI values were −0.0775, 0.0401 and 0.0495 for TC, UCS and LCS, respectively. Similar differences were observed in an additional analysis of a single row with one cultivar. Local and vertical variability analyses confirmed considerable spectral heterogeneity within the canopy. These findings suggest that measurements from different canopy positions provide additional information about vineyard canopy variability, although cultivar, row characteristics, illumination, and measurement geometry may also influence the observed differences.

Keywords: precision viticulture; vineyard monitoring; remote data acquisition

Academic Editor: Ray E. Sheriff

Received: 22 September 2026
Revised: 14 November 2026
Accepted: 16 November 2026
Published: 23 November 2026

Copyright: © 2026 by the authors. Licensee MDPI, Basel, Switzerland. This article is an open access article distributed under the terms and conditions of the Creative Commons Attribution (CC BY) license.

1. Introduction

Innovative agricultural methods combine technological solutions in which environmental and plant observations are carried out in parallel, enabling the recording and analysis of large amounts of data in real time. This makes it possible to observe and digitally reconstruct individual plants, as well as individual plant organs and their immediate environment. In agriculture, a data acquisition system (DAS) is a technological framework designed and built to capture real-time environmental and crop-related data from multiple sources such as soil sensors, weather stations, plant morphological and physiological sensors, machine sensors, and remote sensing platforms. In most cases, a DAS includes sensors and measurement devices, signal conditioning units, data loggers or microcontrollers, communication modules and software interfaces [1,2]. In Agriculture 5.0, its importance is undoubted as a DAS enables real-time monitoring of crop status and field conditions, early detection of environmental or biotic stress such as drought, nutrient deficiency, or the effects of pests or diseases, precise variable-rate applications (for example fertilization, irrigation, pesticide application), improved yield prediction, documentation and traceability for sustainability and certification, and data-driven farm management decisions [3–5].

Remote and proximal sensing are essential components of a DAS to get reliable data about plant morphology, physiology, yield and biomass. For this reason, RGB, multispectral and hyperspectral imaging are core parts of these systems. Spectral information from these monitoring processes is usually represented by vegetation indices (VI), which are unitless values derived from simple mathematical calculations from single-waveband reflectance. The most frequently applied VI is the normalized difference vegetation index (NDVI), which is strongly correlated with plant physiological status and can therefore help identify nutrient deficiency, drought stress, and frost damage [6,7]. Although this multispectral vegetation index has numerous applications, other indices are also available that provide plant physiology data by evaluating multiple wavelengths simultaneously. For example, the photochemical reflectance index (PRI) was originally introduced as a narrow-band "physiological reflectance index", to detect rapid changes in the xanthophyll cycle and photosynthetic light-use efficiency [8]. Although the initial terminology emphasized its physiological relevance, the term "photochemical reflectance index" (PRI) soon became standard, reflecting the index's strong mechanistic link to photochemical quenching processes. Besides the narrowband indices, several RGB-based VIs are available, providing low-cost monitoring solutions using digital cameras, smartphones or flatbed scanners and provide valuable information [9].

Although the NDVI is the most widely used structural vegetation index, which shows correlation with canopy density, biomass, and vigor, it has certain limitations such as saturation caused by dense canopies and a slow response to rapid plant physiological changes. In contrast, PRI reflects short-term variations in the light-use efficiency of the photosynthetic apparatus, but it requires narrowband spectral measurements. While RGB-based indices rely on broadband reflectance and have a high resolution, they are limited to the visible part of the spectrum and are sensitive to illumination and surface effects. Therefore, combining structural (NDVI), functional (PRI) and color-based (RGB) metrics provides a more robust and comprehensive assessment of canopy status and its spatial variability.

Vineyards in most cases consist of corridor-like rows and inter-rows. The rows are built up by the structural elements of the plants in more woody parts such as the trunk, arm, and pruning positions. During bud burst, shoots arise from the winter and hidden buds. Shoot growth shows a sigmoid curve and is affected by several factors such as climatic parameters, soil depth, and water and nutrient content, as well as viticultural practices such as pruning-defined bud-load and further canopy management actions [10–13].

https://doi.org/10.3390/agriengineering8120507

Unlike most horticultural or forest plants, the grapevine (*Vitis vinifera* L.) is liana-like. Considering that bud break in the Northern Hemisphere starts in April and shoot growth stops in early autumn, the age difference between basal and apical leaves may reach 3 to 5 months. The basal leaves, located on the lower part of the shoot, are the oldest, while the newly formed leaves on the top of the shoot are the youngest [13,14]. During shoot growth, new leaves are initiated by the apical meristem; consequently, leaves located at different positions along the shoot exhibit distinct morphological and physiological characteristics. This phenomenon is reflected in plant morphology, physiology, optical properties, and reflectance. For example, it has been shown that leaf position (age) significantly influences stomatal quantitative properties [15]. Moreover, leaf chlorophyll content also differs along the shoot and is influenced by leaf age [16]. It has also been reported that leaf age and phenological stage influence the characteristics of the photosynthetic apparatus of the grapevine leaf [17]. Not only does the regular plant physiology differ along the shoot, but abiotic stress symptoms such as nutrient deficiency can also have a specific location [18,19].

To better understand the variability characteristic of the entire canopy resulting from the above morphological and plant physiological characteristics, technical solutions are needed that examine the reflectance of the canopy not as a whole but divided into sectors. To achieve this goal, the aim of this study is to utilize a mobile sensor data system with multiple sensors at different sections of the canopy. The measurement setup is based on the DisDAQ (Distributed Data Acquisition and Algorithms Quiver) system [20] which is a flexible and modular measurement system. It connects NDVI and PRI sensors, as well as an RGB camera and a GPS module. The whole setup can be freely moved through the vineyard to acquire valuable canopy data while synchronously tracking the position within the vineyard. The measurement data is stored locally but can also be streamed into a cloud storage database if wireless connectivity is available.

2. Materials and Methods

2.1. Sensor System Description

In this study, NDVI and PRI sensors were integrated into the DisDAQ (Distributed Data Acquisition and Algorithms Quiver) system in version 3.4.1. The SRS NDVI and PRI sensors (METER Group Inc., Pullman, WA, USA) are two-band radiometers with central wavelengths of 650 and 810 nm for NDVI and 532 and 570 nm for PRI, respectively, with a 10 nm full-width half-maximum bandwidth. The field-stop sensors used for canopy measurements have a 36° field of view, while the hemispherical sensors used as upward-looking reference sensors have a 180° field of view. According to the manufacturer, the sensors are calibrated against a NIST-traceable transfer standard [21].

The sensor system hardware setup consisted of a custom-built sensor frame carrying multiple sensing modalities. The overall system structure is shown in Figure 1. Hemispherical NDVI and PRI reference sensors were mounted horizontally and oriented upward to capture incoming radiation and provide environmental baseline measurements. Downward-facing NDVI and PRI sensors were co-located on the same horizontal structure to measure reflectance at the top of the canopy (TC). Additional NDVI and PRI sensor pairs were mounted on the vertical section of the frame at two distinct heights to capture lateral canopy variability. These sensors recorded reflectance from the upper canopy side (UCS) and lower canopy side (LCS, corresponding to the bunch zone). This configuration enables simultaneous multi-angular and multi-layer assessment of canopy optical properties. An RGB camera was integrated into the system to capture visual information on canopy structure and color characteristics, complementing the spectral indices, although in this study, RGB information was not evaluated. A GPS module was included to provide

georeferenced measurements, enabling spatial alignment of all sensor data along the vineyard rows.

As already mentioned in the Introduction, the DisDAQ platform is used for sensor data acquisition and storage. DisDAQ is a flexible, scalable measurement platform designed for synchronized acquisition and processing of data from spatially distributed sensors. It enables modular sensor integration, time-synchronized data acquisition, and edge-based preprocessing.

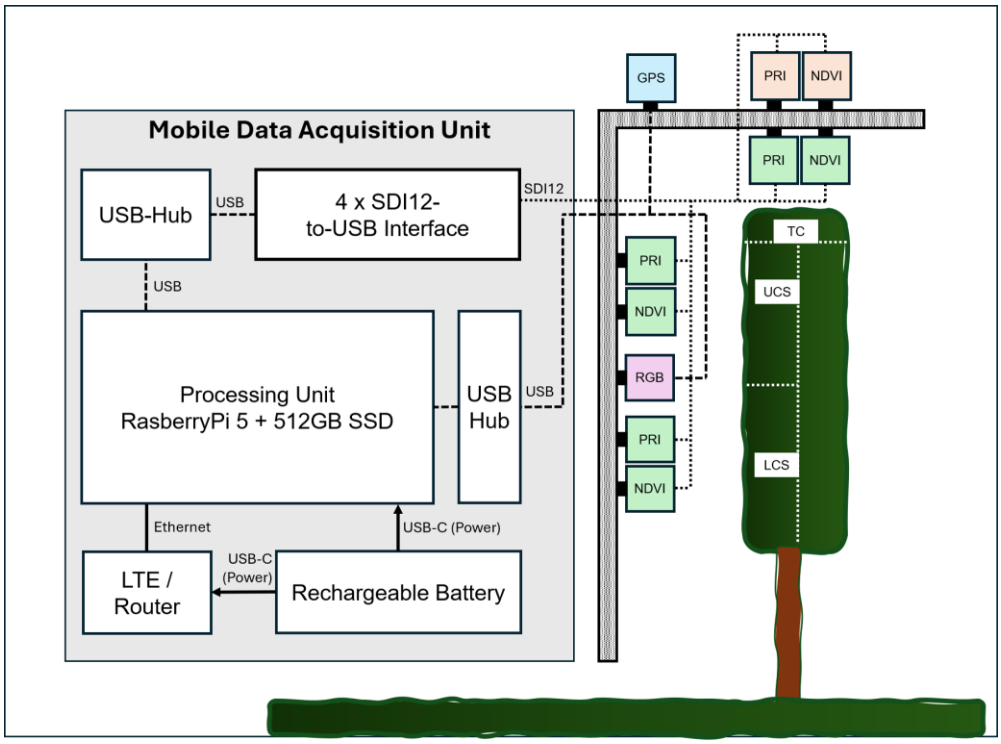

Figure 1. Block diagram and DisDAQ sensor layout of the on-the-go remote sensing system for canopy monitoring. The architecture includes a Raspberry Pi processing unit with 512GB SSD, networking components (modem, switch, router), and power management. The sensor array consists of a GPS module, along with PRI and NDVI sensors and RGB camera positioned at different canopy heights (TC: top canopy, UCS: upper canopy section, LCS: lower canopy section).

On this device, the DisDAQ software is deployed as a local K3s Kubernetes cluster [22,23], hosting dedicated applications for sensor data acquisition, local data storage in an InfluxDB database [24], and downstream processing of the recorded raw data for subsequent evaluation. Communication between all software components is realized via the Robot Operating System 2 (ROS2) framework [25,26], enabling structured data exchange and consistent timestamp synchronization across the system. The platform fully supports local operation independent of network availability, while optionally allowing measured data to be transmitted to external cloud-based databases through wireless communication interfaces such as WLAN or 5G. The entire setup is battery-powered and designed for mobile field deployment, providing an autonomous operating time of approximately 6 to 8 h under typical measurement conditions. All hardware components except the sensors and the GPS antenna were integrated into a portable enclosure. The setup of the mobile data acquisition unit is shown in Figure 2.

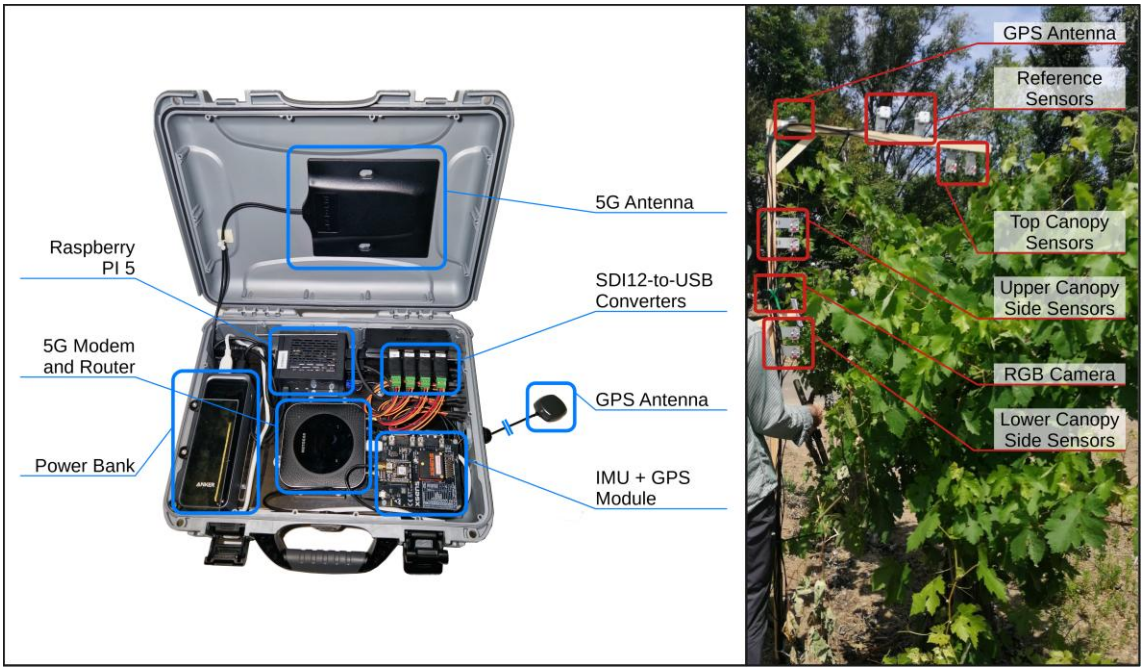

Figure 2. System setup of the mobile data acquisition unit, illustrating the hardware components housed in a portable enclosure on the left side. The right side illustrates sensor array consisting of the GPS antenna, RGB camera, and pairs of PRI and NDVI sensors for top canopy, upper canopy side, lower canopy side and reference measurements.

2.2. Sensors and Interfaces

The sensor setup used in this study comprised NDVI sensors, PRI sensors, SDI-12 bus adapters, an RGB camera, and a GPS module. These sensors were integrated into the existing mobile measurement platform DisDAQ through dedicated communication interfaces, enabling spatially resolved canopy measurements together with continuous position tracking during field operation.

The NDVI and PRI sensors communicate via the SDI-12 protocol, which is commonly used in environmental monitoring applications because of its robustness and suitability for distributed field sensors. To connect these sensors to the processing unit, SDI-12-to-USB converters were employed. Each converter interfaced one pair of optical sensors (one PRI and one NDVI sensor) with the acquisition system, providing a practical and modular solution for integrating multiple commercially available sensors into the mobile platform. This interface structure also allowed the sensor data to be handled uniformly within the overall acquisition workflow.

Although the bus is capable of handling more than two sensors, this structure was chosen to optimize the measurement intervals of the overall system. Since the system was designed for on-the-go measurements in vineyard rows, the interface configuration had to support sufficiently dense spatial sampling along the travel path. The achievable acquisition rate was therefore not only determined by the sensor characteristics themselves but also by the communication behavior of the shared SDI-12 buses. In particular, the optical sensors require significant measurement time during which bus access remains occupied. For this reason, the hardware and interface design had to account for the fact that multiple sensors connected to the same bus cannot be queried fully independently. Rather than discussing these timing constraints in detail here, the present section focuses on the physical and logical integration of the sensors, while the consequences for polling order, effective sampling intervals, and timestamp alignment are addressed in the following section.

In addition to the optical sensors, a combined GPS and inertial measurement module (MTi-670 GNSS/INS from Xsens Technologies B.V., Enschede, Netherlands) was

connected via a dedicated USB interface. Unlike the SDI-12-based sensors, the GPS unit operated independently of the shared sensor buses and delivered position information continuously during field measurements. This allowed each spectral observation to be assigned to a spatial coordinate along the vineyard rows, forming the basis for the georeferenced analysis of canopy variability. The module was selected because it was already available, had demonstrated reliable performance in previous projects, and was fully integrated into the DisDAQ platform. However, lower-cost alternatives are available, ranging from conventional multi-GNSS receivers providing meter-level positioning accuracy to RTK-capable receivers offering centimeter-level accuracy when suitable correction data are available. No external high-precision GNSS correction service was used during the measurements presented in this study. The combination of spectral sensing and positional tracking was essential for relating local reflectance differences to within-row spatial structure. The detailed sensor interface structure is shown in Figure 3.

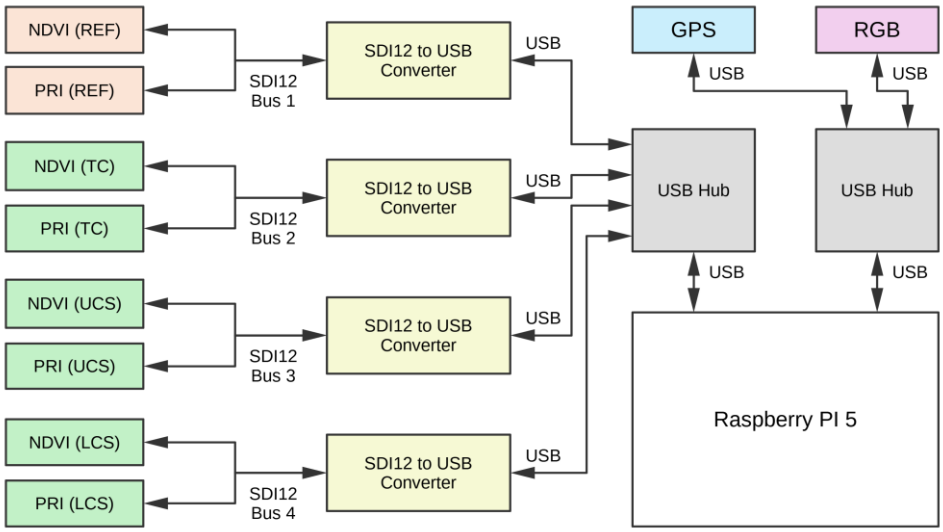

Figure 3. Detailed sensor interface structure showing the four SDI-12 buses and the dedicated converters to enable simultaneous data acquisition of all NDVI or PRI sensors (alternating). The SDI-12 converters are connected to the RaspberryPi 5 using a USB hub.

2.3. Data Bus and Sensor Timing

The NDVI and PRI sensors were connected to the acquisition system via SDI-12 adapters, with two sensors sharing one bus adapter. Since SDI-12 communication is sequential, only one sensor transaction can be executed on a given bus at a time. According to the sensor specifications, the maximum response time for one measurement is approximately 650 ms. During this period, the respective SDI-12 bus remains occupied, so the second sensor connected to the same adapter cannot be triggered simultaneously. Consequently, sensors sharing one bus had to be read out consecutively rather than in parallel. To enable a synchronous readout of all sensors of the same type (NDVI and PRI), each bus connects exactly one NDVI and one PRI sensor as illustrated in Figure 3. This configuration enabled quasi-simultaneous acquisition of each vegetation index across all four measurement positions, while maintaining sequential communication between the NDVI and PRI sensors sharing an individual bus.

The polling interval of the DisDAQ system was set to 1500 ms. This interval was chosen to exceed the maximum sensor response time and thereby avoid communication conflicts or bus collisions during repeated measurements. Under these conditions, each adapter could complete one sensor query safely before the next polling cycle was initiated. This interval was used to calculate the average spatial VI measurement interval reported

in Table 1. Since NDVI and PRI measurements were acquired in alternating polling cycles, each individual sensor was queried every 3000 ms, corresponding to a nominal acquisition rate of approximately 0.33 Hz per sensor.

Table 1. Measurement quality and characteristics parameters of four rows in two vineyards each.

Row	M1L1	M1L2	M1L3	M1L4	M2L1	M2L2	M2L3	M2L4
Measurement duration (s)	510	392	383	343	191	234	187	177
Expected meas. points GPS	342	262	256	230	128	157	126	119
Actual meas. points GPS	342	262	256	230	128	157	126	119
Loss GPS	0	0	0	0	0	0	0	0
Jitter GPS (ms)	±111	±113	±119	±112	±109	±112	±108	±118
Distance (m)	192.9	196.0	196.1	193.4	137.1	135.9	135.9	134.9
Average velocity (m/s)	0.38	0.50	0.51	0.56	0.72	0.58	0.73	0.76
Average spatial VI measurement interval (m)	0.57	0.75	0.77	0.84	1.08	0.87	1.1	1.14
Expected meas. points 4×PRI + 4×NDVI	1368	1048	1024	920	512	628	500	476
Actual meas. points 4×PRI + 4×NDVI	1368	1048	1024	920	512	628	500	476
Loss PRI + NDVI	0	0	0	0	0	0	0	0
Jitter maximum PRI + NDVI (ms)	± 3.68	± 3.46	± 7.33	± 5.39	± 3.83	± 3.61	±3.36	±3.53

However, because the individual SDI-12 adapters were themselves addressed sequentially within the DisDAQ workflow, measurements from different sensors were not recorded at exactly the same instant. Instead, small timestamp offsets occurred between the individual sensor readings within one acquisition cycle. This jitter occurred due to scheduling limitations of the host operating system and container execution.

To enable joint evaluation of the multi-sensor data, these temporally offset measurements were synchronized during post-processing. The recorded timestamps were adjusted to a common global time base, consistent with the synchronized acquisition concept of the DisDAQ platform. This procedure allowed the sensor data to be treated as quasi-simultaneous observations at each measurement position along the vineyard rows, while preserving the practical advantages of the SDI-12-based multi-sensor setup.

2.4. Experimental Plot and Trial Measurement

The sensor system was tested at the research station of the Hungarian University of Agriculture and Life Sciences, in Kecskemét, Hungary. The station is located in the Kunság wine region. The Kunság wine region is the largest wine-producing area in Hungary, located in the central and southern parts of the Great Hungarian Plain. Its climate is warm and relatively dry, with a high number of sunshine hours and uneven, often limited annual precipitation. The region is characterized predominantly by light, sandy soils with good drainage capacity that warm up quickly but have low water-holding capacity. The flat topography and continental climate result in considerable temperature fluctuations and frequent drought periods. These ecological conditions favor early-ripening and aromatic grape varieties while requiring careful water and nutrient management practices.

Test runs were conducted in June 2025 between berry set and veraison in two experimental vineyards (M1 and M2), with four rows (L1 to L4) in each vineyard. The rows were oriented NW-SE, and the training system and grapevine cultivar were different. To test the system's sensitivity, runs were carried out both in complete rows and in rows where a randomly selected percentage of plants was missing.

2.5. Vegetation Indices and Statistical Evaluation

NDVI and PRI were calculated from the raw sensor data. Furthermore, illumination-corrected NDVI and PRI were calculated as shown in Equations (1)–(4):

$$\mathrm{NDVI} = \frac{\rho 810 - \rho 650}{\rho 810 + \rho 650} \quad (1)$$

$$\mathrm{PRI} = \frac{\rho 532 - \rho 570}{\rho 532 + \rho 570} \quad (2)$$

$$\mathrm{NDVI} * = \frac{\frac{\rho 810_{Down}}{\rho 810_{Up}} - \frac{\rho 650_{Down}}{\rho 650_{Up}}}{\frac{\rho 810_{Down}}{\rho 810_{Up}} + \frac{\rho 650_{Down}}{\rho 650_{Up}}} \quad (3)$$

$$\mathrm{PRI} * = \frac{\frac{\rho 532_{Down}}{\rho 532_{Up}} - \frac{\rho 570_{Down}}{\rho 570_{Up}}}{\frac{\rho 532_{Down}}{\rho 532_{Up}} + \frac{\rho 570_{Down}}{\rho 570_{Up}}} \quad (4)$$

Hemispherical reference NDVI and PRI sensors were used to normalize the canopy sensor readings and illumination-normalized NDVI (NDVI*) and illumination-normalized PRI (PRI*) were calculated. Raw and normalized data were compared according to Pearson correlation. As the normalized data for both NDVI and PRI showed high correlation with the raw data, in the further evaluation, the raw data were involved.

For descriptive statistical evaluation, median and interquartile ranges (due to the non-normal distribution of the data) were calculated for NDVI and PRI at the three canopy sections (TC, UCS, LCS, see Figure 1). Local variability along the rows was quantified using the absolute differences between consecutive measurements. For NDVI and PRI, the absolute difference between adjacent observations was calculated as $\Delta x_i = |x_{i+1} - x_i|$, where x_i denotes the value of the vegetation index at the i-th measurement point.

Vertical differences between canopy sections (TC, UCS, LCS) were quantified using the absolute differences between vegetation index values measured simultaneously at the different positions. For each measurement point, the absolute difference was calculated between the TC, UCS and LCS as $|X_{TC} - X_{UCS}|$, $|X_{TC} - X_{LCS}|$, and $|X_{UCS} - X_{LCS}|$. This approach provides a direction-independent measure of vertical canopy contrast, capturing instantaneous differences in canopy structure and physiological status. Due to the non-normal distribution of the data, differences in vegetation index values among canopy positions were evaluated using the Kruskal–Wallis test followed by Bonferroni-corrected Dunn's post hoc test. The same statistical procedure was applied both to the complete pooled dataset and, as an additional sensitivity analysis, to the M2L3 dataset representing a single row with a single cultivar, in order to assess whether the differences among canopy positions were also detectable within a more homogeneous subset of the data.

To evaluate canopy variability, Shannon entropy was calculated for each section. Shannon entropy was calculated based on the distribution of vegetation index values across 20 bins for NDVI and 8 bins for PRI. Relative frequencies were used to compute entropy values, which were further normalized by the maximum possible entropy. Statistical evaluation was carried out in PAST version 4.17c [27].

3. Results

This section presents the results obtained during the trial measurements conducted at the Research Station of the Hungarian University of Agriculture and Life Sciences in Kecskemét, Hungary. The results include both an evaluation of system operation under

field conditions and exemplary sensor data illustrating the spectral variability of the vineyard canopy recorded during the trial measurements.

3.1. Evaluation of Measurement Data

The first evaluation concerned the quality of the measurement data. As already discussed, the trial measurements were split into four rows for each of the two vineyards. For each row, measurement quality and performance parameters were analyzed. Measurement duration, measurement point loss, distance, average velocity, and other characteristics for each row are shown in Table 1. It summarizes the main measurement quality and acquisition characteristics for the four recorded rows in each of the two vineyards. For every row, the table reports the measurement duration, traveled distance, average movement velocity, expected and actual numbers of measurement points for GPS and optical sensing, as well as the corresponding temporal jitter values. Together, these parameters provide an overview of the operational stability and completeness of the mobile data acquisition during the field trials. No data loss was observed in any of the measurement runs, neither for the GPS data nor for the PRI and NDVI sensor readings. The actual number of recorded measurement points matched the expected number in all cases, indicating stable communication and reliable acquisition performance during the trials. This result is consistent with the cable-based sensor integration used in the DisDAQ system, which ensured robust signal transmission under field conditions. The GPS jitter remained within a narrow range of approximately ±108 to ±119 ms across all rows, while the maximum jitter of the PRI and NDVI measurements ranged between ±3.36 and ±7.33 ms. These values indicate a temporally stable acquisition process and confirm that the configured polling and synchronization strategy was adequate for mobile vineyard measurements.

The recorded distances were highly consistent within each vineyard. In vineyard M1, all four rows showed lengths of approximately 193 to 196 m, whereas in vineyard M2 the corresponding distances ranged from approximately 135 to 137 m. This agreement reflects the comparable row lengths within each vineyard and supports the plausibility of the GPS-based trajectory reconstruction. Differences in measurement duration and average velocity between rows are mainly attributable to varying movement speeds during the field runs rather than to technical limitations of the acquisition system.

Figure 4 illustrates the measurement paths recorded in vineyard M1. Each path corresponds to a different vine row, including rows planted with different grapevine cultivars. The measurement movement direction varied between runs: Rows 1 and 3 were measured from northeast to southwest, whereas Rows 2 and 4 were measured in the opposite direction, from southwest to northeast. During all runs, the sensor system was oriented toward the left-hand side relative to the direction of movement, so that the observed canopy side depended on the driving direction. This measurement design enabled comparison between rows differing in training system and cultivar. In addition, to evaluate the sensitivity of the system under variable field conditions, measurements were conducted both in continuous rows and in rows with missing plants.

Figure 5 illustrates the measurement paths recorded in vineyard M2. The movement directions were identical to those used in vineyard M1: Rows 1 and 3 were measured from northeast to southwest, whereas Rows 2 and 4 were measured from southwest to northeast. In contrast to vineyard M1, however, the orientation of the measurement system was changed from the left-hand side to the right-hand side relative to the direction of movement for Rows 2 and 3. As a result, Rows 2 and 3 correspond to measurements of the same vine row acquired from opposite directions and opposite canopy sides. This setup enabled an assessment of the influence of sensor orientation relative to the canopy as well as the effect of row traversal direction on the recorded data. Furthermore, Rows 2 and 3 appear very close to each other in the spatial representation, reflecting that both measurement

runs followed the same vine row but from different sides. At the same time, the GPS data quality was sufficient to distinguish not only between adjacent vine rows but also between repeated measurements of the same row from opposite sides. This confirms that the positional information was accurate enough to reliably assign the spectral data to the correct row and canopy side. Overall, this measurement arrangement allowed the same vineyard structures to be evaluated from both sides and under reversed travel directions, thereby improving the representativeness and interpretability of the recorded spatial patterns.



Figure 4. GPS tracks recorded during the field testing of the DisDAQ-agri mobile data acquisition system of the four measurement rows through vineyard M1.



Figure 5. GPS tracks recorded during the field testing of the DisDAQ-agri mobile data acquisition system for the four measurement rows through vineyard M2. Note that Rows 2 and 3 correspond to measurements of the same vine row, acquired from opposite directions and opposite canopy sides.

The GPS data quality proved sufficient to reliably reconstruct the measurement trajectories within vineyards M1 and M2. In particular, the recorded coordinates allowed clear identification of the individual vine rows and, during this measurement run, even enabled discrimination between the two sides of the vine row. This level of positional

accuracy is important for the interpretation of the sensor data, as it ensures that differences in spectral response can be assigned not only to a specific row but also to the respective canopy side observed during the pass. Thus, the GPS measurements provided an adequate spatial basis for georeferencing and contextualizing the acquired reflectance data.

3.2. Spectral Variability of the Canopy Sections

The analysis was performed separately for structural (NDVI) and physiological (PRI) indices (Table 2). Vegetation indices were evaluated based on their mean values and variability among canopy sections. Median NDVI values were 0.4329, 0.3221 and 0.6161 for TC, UCS and LCS as shown in Figure 6. Statistical analysis revealed significant differences between canopy sections ($p < 0.01$). PRI values also differed significantly ($p < 0.01$) among sections, with the lowest median value observed at TC (−0.0775), followed by UCS and LCS (0.0401 and 0.0495, respectively) as shown in Figure 7. The statistical evaluation was conducted across all measurements.

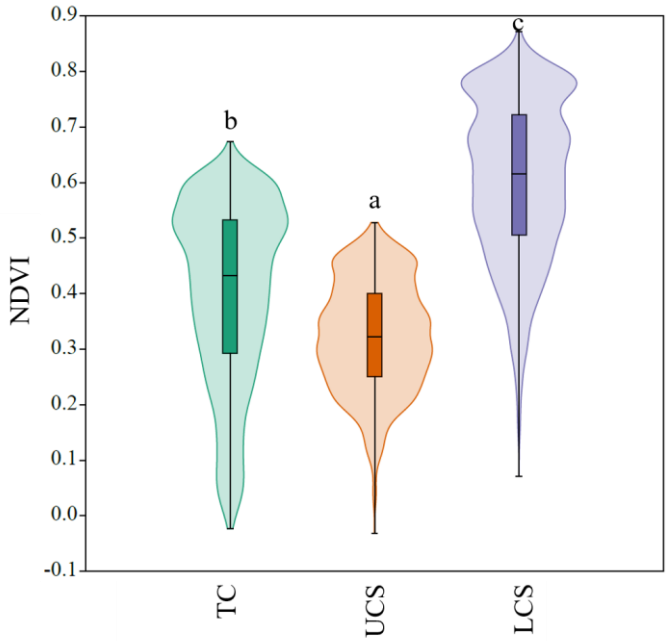

Figure 6. NDVI values measured in the three sections of the canopy across all measurements. Significant differences among canopy sections were detected using the Kruskal–Wallis test, followed by Bonferroni-corrected Dunn's post hoc test ($p < 0.01$).

Local variability, expressed as the absolute difference between consecutive measurements, also showed significant ($p < 0.01$) differences among canopy sections (Table 2). For NDVI, the lowest variability was observed in UCS (0.0068), followed by LCS (0.0092) and TC (0.0111). For PRI, differences were also significant ($p < 0.01$). The lowest values were recorded in UCS (0.0048), followed by TC (0.0070), while the highest variability was observed in LCS (0.0081).

Vertical differences between canopy sections, calculated as absolute differences between simultaneous measurements, showed significant differences for all NDVI comparisons (TC–UCS, TC–LCS and UCS–LCS; $p < 0.01$). The smallest differences were observed between TC and UCS (0.1413), while the largest occurred between UCS and LCS (0.2832). Similar patterns were observed for PRI, where all pairwise comparisons differed significantly ($p < 0.01$). The highest differences were detected between TC and LCS (0.1248), while the lowest were observed between UCS and LCS (0.0532) (Table 2).

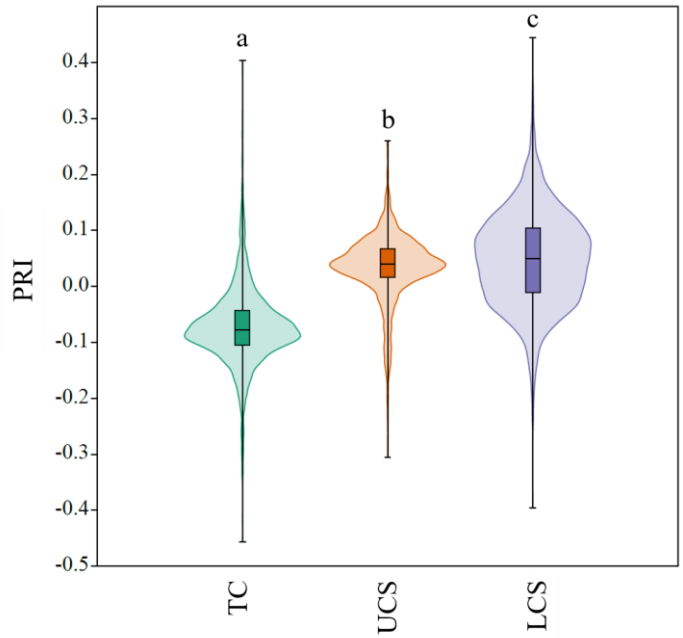

Figure 7. PRI values measured in the three sections of the canopy across all measurements. Significant differences among canopy sections were detected using the Kruskal–Wallis test followed by Bonferroni-corrected Dunn's post hoc test ($p < 0.01$).

Shannon entropy analysis of NDVI indicated the highest variability in TC (H_{norm} = 0.9340; H = 2.7979), followed by UCS (H_{norm} = 0.8780; H = 2.6301) and LCS (H_{norm} = 0.8684; H = 2.6016). In contrast, PRI exhibited an opposite trend, with the lowest entropy observed in TC (H_{norm} = 0.4594; H = 0.9553), while higher values were recorded in UCS and LCS (H_{norm} = 0.5937; H = 1.2346 and H_{norm} = 0.5921; H = 1.2312, respectively) (Table 2).

To examine whether the differences among canopy measurement positions were also detectable within a more homogeneous subset of the dataset, an additional analysis was performed using measurements from a single row consisting of a single cultivar. A significant difference in NDVI was detected among canopy positions (Kruskal–Wallis test, $p < 0.001$). Bonferroni-corrected Dunn's post hoc comparisons showed that LCS differed significantly from both TC and UCS ($p < 0.001$), whereas no significant difference was detected between TC and UCS ($p = 1.000$). Overall, the additional analysis showed that differences among canopy sections were also detectable when a single row with one cultivar was evaluated separately.

Table 2. Descriptive statistics of NDVI and PRI values, local and vertical differences, and Shannon entropy across canopy sections. Different letters indicate significant differences at $p < 0.01$ using the Kruskal–Wallis test followed by Bonferroni-corrected Dunn's post hoc test.

	NDVI	**PRI**	**NDVI_delta_xi**	**PRI_delta_xi**	**NDVI**		**PRI**	
	median	median	median	median	H	H_norm	H	H_norm
TC	0.4329 ^{b}	−0.0775 ^{a}	0.0111 ^{c}	0.0070 ^{c}	2.7979	0.9340	0.9553	0.4594
UCS	0.3221 ^{a}	0.0401 ^{b}	0.0068 ^{a}	0.0048 ^{a}	2.6301	0.8780	1.2346	0.5937
LCS	0.6161 ^{c}	0.0495 ^{c}	0.0092 ^{b}	0.0081 ^{b}	2.6016	0.8684	1.2312	0.5921
TC-UCS	0.1413 ^{a}	0.1174 ^{b}						
TC-LCS	0.1845 ^{b}	0.1248 ^{c}						
UCS-LCS	0.2832 ^{c}	0.0532 ^{a}						

4. Discussion

Variable-rate applications in fertilization, irrigation, or plant protection require detailed monitoring of the plant population to be able to evaluate its variability and act accordingly. Several environmental factors can enhance the differences among the individual plants, such as properties of the soil (depth, structure, nutrient content), topography (elevation, slope, inclination), microclimate (temperature, wind, radiation, precipitation). Moreover, several structural elements and maintenance practices such as rootstock, training system, pruning and canopy management have effects on individual plants that could cause morphological and physiological variation. Although there are several remote and proximal sensing methods available to evaluate this variability, specific solutions are the focus of many agricultural sectors [28–30].

Grapevine is a perennial liana crop, and unlike arable crops, grapevine exhibits not only horizontal (among-plant) variability but also vertical (within-plant) variability arising from ontogeny and heteroblasty. In this study, we introduced an on-the-go sensor system that monitors both the horizontal and vertical spectral variability linked to the most important remote sensing attributes, NDVI and PRI.

We found significant differences between the three canopy sections. The same pattern was also observed when the M2L3 row, consisting of a single cultivar, was evaluated separately, indicating that the observed differences were not only related to the heterogeneity of the pooled dataset. Differences in leaf age and pigment content among canopy positions, as reported in previous studies [16,17], may partly contribute to the observed patterns. However, the measured values can also be influenced by several other factors. Especially at LCS, lower values may result from measurement geometry and incomplete canopy coverage within the sensor field of view, but they can also indicate actual canopy variability caused by missing vines, stress or disease symptoms. Therefore, the differences among canopy sections should not be attributed exclusively to physiological differences within the canopy.

4.1. Future Perspectives—Further Vegetation Indices

Even if the NDVI and PRI are the most promising VIs provided by the sensors used in this study, the data from the four channels: green (532 nm), yellow (570 nm), red (650 nm) and near-infrared (810 nm), allow for calculating further vegetation indices. NDVI has become a standard vegetation index due to its relatively linear relationship with vegetation amount, its bounded and interpretable range, and its widespread adoption in remote sensing studies. Further indices can also be derived from the red and NIR reflectance values.

NDVI has been shown to saturate under moderate-to-high vegetation density, becoming less sensitive to further increases in leaf area index (LAI) due to its normalized formulation [31]. To overcome this limitation, the Wide Dynamic Range Vegetation Index (WDRVI) introduces a as a weighting coefficient to the NIR reflectance, increasing the dynamic range, improving linearity, and enhancing sensitivity under dense canopy conditions. In addition to NDVI, further indices were introduced over the decades. The Infrared Percentage Vegetation Index (IPVI), for example, provides a computationally more efficient and non-negative alternative to NDVI, while remaining linearly equivalent and thus preserving the same information content. Unlike NDVI, the Simple Ratio (SR) is not bounded, which complicates interpretation and comparison across datasets, although it is widely applied in vegetation studies [32,33]. The Modified Simple Ratio (MSR) has been introduced to improve the non-linear behavior of the simple ratio and reduce NDVI saturation, resulting in a more linear and robust relationship with vegetation parameters such as LAI [34].

$$\mathrm{WDRVI} = \frac{a \times \rho 810 - \rho 650}{a \times \rho 810 + \rho 650} \quad (5)$$

$$\mathrm{IPVI} = \frac{\rho 810}{\rho 810 + \rho 650} \quad (6)$$

$$\mathrm{SR} = \frac{\rho 810}{\rho 650} \quad (7)$$

$$\mathrm{MSR} = \frac{\left(\frac{\rho 810}{\rho 650}\right) - 1}{\sqrt{\frac{\rho 810}{\rho 650}} + 1} \quad (8)$$

The above-mentioned indices were developed to address key limitations of NDVI, including its saturation at high vegetation density and its sensitivity to background reflectance. Furthermore, numerous additional vegetation indices are available using the data from the four channels: green (532 nm), yellow (570 nm), red (650 nm), and near-infrared (810 nm), as summarized in dedicated databases such as the Index Database (IDB) [35]. Additional vegetation indices may provide further information; however, their practical applicability should be validated under field conditions. Future studies should also evaluate the effects of canopy architecture, illumination conditions and sensor-to-canopy geometry on the measured signals.

4.2. Future Perspectives—RGB and IR Sensors

The combination of RGB and NIR or additional sensors gives a deeper insight into biophysical parameters, biomass and vegetation density [36]. For this reason hardware was developed to allow the integration of more sensors into the system. Previous studies reported that RGB sensors provide valuable information about plant morphology and plant status-related pigment concentrations [37,38]. Prediction of chlorophyll concentration is of high importance not only in plant physiological monitoring but also in plant pathological investigations. Moreover, nutrient deficiencies, soil properties unsuitable or unfavorable for cultivation, and pests and diseases usually have visible symptoms that can be detected by RGB sensors. InfraRed sensors are also widely used in precision agriculture; for example, low-cost thermal sensors provide valuable information for water stress monitoring through Crop Water Stress Index (CWSI) estimation [39]. Nowadays, climate change is shifting viticulture toward irrigation in many regions. Thus, on-the-go monitoring of water status is considered a valuable opportunity.

4.3. Future Perspectives—Horizontal Orientation

The present study focused on evaluating vineyard canopy reflectance variability using a vertically oriented sensor configuration. While viticulture represents a key sector of high-value crop production, precision agriculture technologies and on-the-go sensing systems are more widely adopted in arable farming. In these systems, sensor networks are commonly used to assess spatial variability in crop status and support site-specific management practices.

The growing importance of on-the-go sensing is reflected in several established technologies designed for biomass and canopy development monitoring [40] and for nitrogen status assessment, including systems such as Yara N-Sensor, Crop Circle, Trimble GreenSeeker, and Fritzmeier ISARIA [41–43].

In the present study, the sensor system was configured primarily for vertical canopy assessment, including sensors targeting the top of the canopy (TC), upper canopy side (UCS) and lower canopy side (LCS), complemented by reference sensors. However, the

same system architecture allows for flexible reconfiguration. A horizontal sensor orientation could provide an optimal setup for monitoring spatial variability in arable crops, vegetable production systems, cover crops or natural vegetation, where canopy structure is more homogeneous and horizontally distributed.

These perspectives highlight the broader applicability of the developed sensor system beyond viticulture, supporting its potential use in a wide range of agricultural environments.

5. Conclusions

On-the-go remote sensing represents an important component of precision agriculture and variable-rate applications. Due to the specific structural characteristics of vineyards, measurement approaches capable of capturing variability at different canopy levels are required. In this study, a DisDAQ-based mobile sensor system integrating NDVI and PRI sensors with GNSS/INS-based positioning was developed and evaluated under field conditions. Measurements were conducted along eight vineyard rows across two experimental vineyards, covering a total distance of approximately 1.32 km. The system enabled the spatially resolved acquisition of vegetation indices at three canopy levels (top, upper side, and lower side), with a minimum spatial sampling interval of approximately 0.57 m.

The field trials demonstrated reliable data acquisition, with no recorded loss of GPS, NDVI, or PRI measurement data. Furthermore, the analysis revealed statistically significant differences in vegetation indices among the investigated canopy levels, demonstrating the importance of considering vertical canopy variability.

Overall, the results demonstrate the feasibility of mobile, multi-level vegetation index acquisition under practical vineyard conditions. By providing vertically differentiated spectral information that is not directly accessible through conventional top-view satellite or UAV observations, the proposed approach offers a complementary sensing method with potential applications in precision viticulture and site-specific vineyard management.

Author Contributions: Conceptualization and system design, L.B.H., T.D., F.H. and P.B.-P.; software and investigation (data acquisition), R.S., R.R. and P.B.-P.; data preparation, analysis, and visualization, L.B.H., R.S. and P.B.-P.; resources, D.Á.N.S.; writing—original draft preparation, R.O., B.N., T.D., L.B.H., L.M., P.M., F.H. and P.B.-P.; writing, review and editing, L.B.H., T.D., L.M., P.M., F.H. and P.B.-P. All authors have read and agreed to the published version of the manuscript.

Funding: This work has been supported in part by the Agri-Digital Growth Central Europe Interreg project (CE0200761) and the COMET Center of the Linz Center of Mechatronics (LCM) funded by the Austrian federal government and the federal state of Upper Austria.

Institutional Review Board Statement: Not applicable.

Informed Consent Statement: Not applicable.

Data Availability Statement: The original contributions presented in this study are included in the article. Further inquiries can be directed to the corresponding author.

Acknowledgments: During the preparation of this manuscript, the authors used ChatGPT (GPT-6, OpenAI) for language editing, improving readability, and discussing potential statistical and data-analysis approaches. The tool was used to support methodological considerations but was not used to perform statistical analyses, process research data, or generate scientific results. All statistical analyses, interpretation of the results, and scientific conclusions were performed, verified, and critically evaluated by the authors. The authors reviewed and edited the final manuscript and take full responsibility for its content.

Conflicts of Interest: The authors L.B.H., F.H., R.S. and R.R. were employed by the company Linz Center of Mechatronics GmbH which is a non-profit research organization. The remaining authors declare that the research was conducted in the absence of any commercial or financial relationships that could be construed as a potential conflict of interest.

Abbreviations

The following abbreviations are used in this manuscript:

5G	Fifth-Generation Mobile Network
CWSI	Crop Water Stress Index
DAS	Data Acquisition System
DisDAQ	Distributed Data Acquisition and Algorithms Quiver
GNSS	Global Navigation Satellite System
GPS	Global Positioning System
IDB	Index Database
INS	Inertial Navigation System
IR	Infrared
LAI	Leaf Area Index
LCS	Lower Canopy Section
NDVI	Normalized Difference Vegetation Index
NIR	Near-Infrared
PRI	Photochemical Reflectance Index
RGB	Red-Green-Blue
ROS2	Robot Operating System 2
SSD	Solid-State Drive
TC	Top Canopy
UCS	Upper Canopy Section
VI	Vegetation Index
WDRVI	Wide Dynamic Range Vegetation Index
WLAN	Wireless Local Area Network

References

1. Zhang, N.; Wang, M.; Wang, N. Precision agriculture—A worldwide overview. *Comput. Electron. Agric.* **2002**, *36*, 113–132. https://doi.org/10.1016/S0168-1699(02)00096-0.
2. Getahun, S.; Kefale, H.; Gelaye, Y. Application of precision agriculture technologies for sustainable crop production and environmental sustainability: A systematic review. *Sci. World J.* **2024**, *2024*, 2126734. https://doi.org/10.1155/2024/2126734.
3. Mulla, D.J. Twenty five years of remote sensing in precision agriculture: Key advances and remaining knowledge gaps. *Biosyst. Eng.* **2013**, *114*, 358–371. https://doi.org/10.1016/j.biosystemseng.2012.08.009.
4. Ammoniaci, M.; Kartsiotis, S.P.; Perria, R.; Storchi, P. State of the art of monitoring technologies and data processing for precision viticulture. *Agriculture* **2021**, *11*, 201. https://doi.org/10.3390/agriculture11030201.
5. Bai, Y.; Liao, Z.; Shang, J.; Gan, W.; Kong, X.; Wei, X. A review on real-time plant monitoring sensors for smart agriculture. *Chem. Eng. J.* **2025**, *523*, 168868. https://doi.org/10.1016/j.cej.2025.168868.
6. McCloskey, L.; Sams, B.; Harris, J.L.; Salie, M.; Striegler, R.K.; Sanchez, L.; Dokoozlian, N. Relationships between freeze damaged vines and imagery from satellites and unmanned aerial vehicles in California vineyards. *Precis. Agric.* **2023**, 955–961. https://doi.org/10.3920/978-90-8686-947-3_120.
7. Vera-Esmeraldas, A.; Pizarro-Oteíza, S.; Labbé, M.; Rojo, F.; Salazar, F. UAV-Based Spectral and Thermal Indices in Precision Viticulture: A Review of NDVI, NDRE, SAVI, GNDVI, and CWSI. *Agronomy* **2025**, *15*, 2569. https://doi.org/10.3390/agronomy15112569.
8. Gamon, J.A.; Penuelas, J.; Field, C.B. A narrow-waveband spectral index that tracks diurnal changes in photosynthetic efficiency. *Remote Sens. Environ.* **1992**, *41*, 35–44. https://doi.org/10.1016/0034-4257(92)90059-S.
9. Bodor-Pesti, P.; Nguyen, L.L.P.; Nguyen, T.B.; Dam, M.S.; Taranyi, D.; Baranyai, L. LeafLaminaMap: Exploring Leaf Color Patterns Using RGB Color Indices. *AgriEngineering* **2025**, *7*, 39. https://doi.org/10.3390/agriengineering7020039.

10. Winkler, A.J. *General Viticulture*; University of California Press: Berkeley, CA, USA, 1974.
11. Júnior, A.F.N.; Amorim, L.; Savary, S.; Willocquet, L. Modelling the dynamics of grapevine growth over years. *Ecol. Model.* **2018**, *369*, 77–87. https://doi.org/10.1016/j.ecolmodel.2017.12.016.
12. Poni, S.; Intrieri, C.; Magnanini, E. Seasonal growth and gas exchange of conventionally and minimally pruned Chardonnay canopies. *Vitis* **2000**, *39*, 13–18.
13. Bodor-Pesti, P.; Taranyi, D.; Deák, T.; Nyitrainé Sárdy, D.Á.; Varga, Z. A review of ampelometry: Morphometric characterization of the grape (*Vitis* spp.) Leaf. *Plants* **2023**, *12*, 452. https://doi.org/10.3390/plants12030452.
14. Chitwood, D.H.; Klein, L.L.; O'Hanlon, R.; Chacko, S.; Greg, M.; Kitchen, C.; Miller, A. J.; Londo, J.P. Latent developmental and evolutionary shapes embedded within the grapevine leaf. *New Phytol.* **2016**, *210*, 343–355. https://doi.org/10.1111/nph.13754.
15. Bodor, P.; Szekszárdi, A.; Varga, Zs.; Baló, B. Investigation of the stomata size and frequency of grapevine (*Vitis vinifera* L.) cultivar 'Kékfrankos'. *COLUMELLA–J. Agric. Environ. Sci.* **2019**, *6*, 29–34. http://doi.org/10.18380/SZIE.COLUM.2019.6.29.
16. Cabello-Pasini, A.; Macías-Carranza, V. Optical properties of grapevine leaves: Reflectance, transmittance, absorptance and chlorophyll concetration. *Agrociencia* **2011**, *45*, 943–957.
17. Sitko, K.; Rusinowski, S.; Pogrzeba, M.; Daszkowska-Golec, A.; Gieroń, Ż.; Kalaji, H.M.; Małkowski, E. Development and aging of photosynthetic apparatus of *Vitis vinifera* L. during growing season. *Photosynthetica* **2020**, *58*, 186–193. https://doi.org/10.32615/ps.2019.107.
18. Rustioni, L.; Grossi, D.; Brancadoro, L.; Failla, O. Characterization of iron deficiency symptoms in grapevine (*Vitis* spp.) leaves by reflectance spectroscopy. *Plant Physiol. Biochem.* **2017**, *118*, 342–347. https://doi.org/10.1016/j.plaphy.2017.06.031.
19. Rustioni, L.; Grossi, D.; Brancadoro, L.; Failla, O. Iron, magnesium, nitrogen and potassium deficiency symptom discrimination by reflectance spectroscopy in grapevine leaves. *Sci. Hortic.* **2018**, *241*, 152–159. https://doi.org/10.1016/j.scienta.2018.06.097.
20. Hörmann, L.B.; Helmel, C.; Putz, V.; Kastl, C. P23-DisDAQ-A Modular and Distributed Measurement and Processing System for Industrial Process Optimization. In Proceedings of the Tagungsband 22. GMA/ITG-Fachtagung Sensoren und Messsysteme 2024, Nuremberg, Germany, 11–12 June 2024; pp. 510–515. https://doi.org/10.5162/sensoren2024/P23.
21. METER Group, Inc. *SRS–Spectral Reflectance Sensor–Operator's Manual*; METER Group, Inc.: Pullman, WA, USA, 2021, p. 34. Available online: https://library.metergroup.com/Manuals/14597_SRS_Web.pdf (accessed on 5 November 2026).
22. K3s Project Authors. K3s–Lightweight Kubernetes. 2026. Available online: https://k3s.io (accessed on 9 June 2026).
23. Koziolek, H.; Eskandani, N. Lightweight Kubernetes Distributions: A Performance Comparison of MicroK8s, k3s, k0s, and MicroShift. In Proceedings of the 2023 ACM/SPEC International Conference on Performance Engineering (ICPE 2023), Coimbra, Portugal, 15–19 April 2023; pp. 17–29. https://doi.org/10.1145/3578244.3583737.
24. *InfluxDB*; InfluxData Inc.: San Francisco, CA, USA, 2026. Available online: https://www.influxdata.com/ (accessed on 9 June 2026).
25. *ROS-Robot Operating System*; Open Robotics: Mountain View, CA, USA, 2026. Available online: https://www.ros.org/ (accessed on 9 June 2026).
26. Maruyama, Y.; Kato, S.; Azumi, T. Exploring the Performance of ROS2. In Proceedings of the 13th International Conference on Embedded Software (EMSOFT '16), Pittsburgh, PA, USA, 1–7 October 2016; pp. 1–10. https://doi.org/10.1145/2968478.2968502.
27. Hammer, Ø.; Harper, D.A.; Ryan, P.D. PAST: Paleontological statistics software package for education and data analysis. *Palaeontol. Electron.* **2001**, *4*, 1–9.
28. Pereyra, G.; Pellegrino, A.; Ferrer, M.; Gaudin, R. How soil and climate variability within a vineyard can affect the heterogeneity of grapevine vigour and production. *OENO One* **2023**, *57*, 297–313. https://dx.doi.org/10.20870/oeno-one.2023.57.3.7498.
29. Vaudour, E.; Costantini, E.; Jones, G.V.; Mocali, S. An overview of the recent approaches to terroir functional modelling, footprinting and zoning. *Soil* **2015**, *1*, 287–312. https://doi.org/10.5194/soil-1-287-2015.
30. Gatti, M.; Garavani, A.; Squeri, C.; Diti, I.; De Monte, A.; Scotti, C.; Poni, S. Effects of intra-vineyard variability and soil heterogeneity on vine performance, dry matter and nutrient partitioning. *Precis. Agric.* **2022,** *23*, 150–177.
31. Gitelson, A.A. Wide dynamic range vegetation index for remote quantification of biophysical characteristics of vegetation. *J. Plant Physiol.* **2004**, *161*, 165–173. https://doi.org/10.1078/0176-1617-01176.
32. Crippen, R.E. Calculating the vegetation index faster. *Remote Sens. Environ.* **1990**, *34*, 71–73. https://doi.org/10.1016/0034-4257(90)90085-Z.
33. Perry Jr, C.R.; Lautenschlager, L.F. Functional equivalence of spectral vegetation indices. *Remote Sens. Environ.* **1984**, *14*, 169–182. https://doi.org/10.1016/0034-4257(84)90013-0.
34. Chen, J.M.; Cihlar, J. Retrieving leaf area index of boreal conifer forests using Landsat TM images. *Remote Sens. Environ.* **1996**, *55*, 153–162. https://doi.org/10.1016/0034-4257(95)00195-6.

35. Henrich, V.; Götze, E.; Jung, A.; Sandow, C.; Thürkow, D.; Gläßer, C. Development of an online indices database: Motivation, concept and implementation. In Proceedings of the 6th EARSeL Imaging Spectroscopy Sig Workshop Innovative Tool for Scientific and Commercial Environment Applications, Tel Aviv, Israel, 16–19 March 2009; pp. 16–18.
36. Giovos, R.; Tassopoulos, D.; Kalivas, D.; Lougkos, N.; Priovolou, A. Remote sensing vegetation indices in viticulture: A critical review. *Agriculture* **2021**, *11*, 457. https://doi.org/10.3390/agriculture11050457.
37. Sánchez-Sastre, L.F.; Alte da Veiga, N.M.; Ruiz-Potosme, N.M.; Carrión-Prieto, P.; Marcos-Robles, J.L.; Navas-Gracia, L.M.; Martín-Ramos, P. Assessment of RGB vegetation indices to estimate chlorophyll content in sugar beet leaves in the final cultivation stage. *AgriEngineering* **2020**, *2*, 128–149. https://doi.org/10.3390/agriengineering2010009.
38. Bodor-Pesti, P.; Taranyi, D.; Nyitrainé Sárdy, D.Á.; Le Phuong Nguyen, L.; Baranyai, L. Correlation of the grapevine (vitis vinifera l.) leaf chlorophyll concentration with rgb color indices. *Horticulturae* **2023**, *9*, 899. https://doi.org/10.3390/horticulturae9080899.
39. Noguera, M.; Millán, B.; Pérez-Paredes, J.J.; Ponce, J.M.; Aquino, A.; Andújar, J.M. A new low-cost device based on thermal infrared sensors for olive tree canopy temperature measurement and water status monitoring. *Remote Sens.* **2020**, *12*, 723. https://doi.org/10.3390/rs12040723.
40. Rosen, L.; Ewing, P.M.; Runck, B.C. RGB-based indices for estimating cover crop biomass, nitrogen content, and carbon: Nitrogen ratio. *Agron. J.* **2024**, *116*, 3070–3080. https://doi.org/10.1002/agj2.21657.
41. Mezera, J.; Lukas, V.; Horniaček, I.; Smutný, V.; Elbl, J. Comparison of proximal and remote sensing for the diagnosis of crop status in site-specific crop management. *Sensors* **2021**, *22*, 19. https://doi.org/10.3390/s22010019.
42. Silva, L.; Conceição, L.A.; Lidon, F.C.; Maçãs, B. Remote monitoring of crop nitrogen nutrition to adjust crop models: A review. *Agriculture* **2023**, *13*, 835. https://doi.org/10.3390/agriculture13040835.
43. Govaerts, B.; Verhulst, N. *The Normalized Difference Vegetation Index (NDVI) Greenseeker (TM) Handheld Sensor: Toward the Integrated Evaluation of Crop Management. Part A-Concepts and Case Studies*; International Maize and Wheat Improvement Center CIMMYT: Mexico City, Mexico, 2010.

Disclaimer/Publisher's Note: The statements, opinions and data contained in all publications are solely those of the individual author(s) and contributor(s) and not of MDPI and/or the editor(s). MDPI and/or the editor(s) disclaim responsibility for any injury to people or property resulting from any ideas, methods, instructions or products referred to in the content.